AGU PUBLICATIONS

JGR

Journal of Geophysical Research: Space Physics

BRIEF REPORT

10.1002/2013JA019512

**Key Points:**
- Simultaneous ground-based conjugate observations of preonset aurora and Pi1-Pi12
- Pi1-Pi12 signatures relavant to the preonset arc evolution
- Interhemispheric similarity/dissimilarity of preonset signatures

**Correspondence to:**
T. Motoba,
tetsuo.motoba@gmail.com

**Citation:**
Motoba, T., S. Ohtani, A. Kadokura, and J. Gjerloev (2014), Interrelationship between preonset auroral and magnetic signatures at a geomagnetically conjugate Iceland-Syowa pair, *J. Geophys. Res. Space Physics*, *119*, 761–769, doi:10.1002/2013JA019512.

Received 2 OCT 2013
Accepted 23 JAN 2014
Accepted article online 29 JAN 2014
Published online 19 FEB 2014

# Interrelationship between preonset auroral and magnetic signatures at a geomagnetically conjugate Iceland-Syowa pair

**T. Motoba[1], S. Ohtani[1], A. Kadokura[2], and J. Gjerloev[1,3]**

[1]Johns Hopkins University Applied Physics Laboratory, Laurel, Maryland, USA, [2]National Institute of Polar Research, Tokyo, Japan, [3]Birkeland Centre for Space Science, University of Bergen, Bergen, Norway

**Abstract** We present the initiation and development of Pi1-Pi2 band pulsations in concert with spatiotemporal evolution of preonset auroral arc during an isolated auroral substorm reported by Motoba et al. (2012), and their interhemispheric similarities/dissimilarities, based on the colocated optical and magnetic field measurements at a geomagnetically conjugate Iceland-Syowa pair. At least ~7 min prior to the auroral expansion onset, the first identifiable signature of preonset arc began with a small-scale (~30–50 km) azimuthal beading. Interestingly, the early development of the visible arc beading for ~3–4 min was not accompanied by any ground magnetic perturbation. Then the bead-like forms in the arc evolved into brighter, larger undulations, eventually developing into the poleward expansion. Such a preonset optical sequence was almost identical at both stations. In the transition from the beads into undulations, Pi2 pulsations were first identified clearly, followed by Pi1 pulsations a few minutes later. Whereas the Pi2 onset was coincident with the initiation of progressive increase of the preonset arc luminosity, the Pi1 onset was associated with a subsequent steep increase. The Pi2 wave cycles superimposed on the magnetic negative bay were well correlated with the preonset arc luminosity time series. These results imply the potential linkage between the ground Pi1-Pi2 signatures in the onset region and the preonset auroral arc processes. Although the Pi1-Pi2 features were generally similar between the two hemispheres, there was also some dissimilarity in their temporal behaviors, which could reflect a small but noteworthy interhemispheric asymmetry in the overhead conjugate preonset aurora.

## 1. Introduction

A well-isolated substorm usually undergoes a characteristic time sequence: growth phase, expansion phase, and recovery phase. Especially, when, where, and how the growth phase transits into the expansion phase (i.e., the sequence of key processes leading to substorm onset) within several minutes has been a major issue of substorm research. Auroral observations are generally considered as the most accurate way of timing the onset signatures and sequences. According to the sequence of auroral substorms first identified by *Akasofu* [1964] based on all-sky camera observations, a sudden brightening (within a few minutes) initially appears in one of the quiet arcs and is also often accompanied by the development of a distinct ray structure. Subsequently, the brightening arc is followed by a rapid poleward expansion, resulting in the formation of a bulge around the midnight sector. Here the term "poleward expansion" or "breakup" has often been used in substorm studies as the start (onset) of an auroral substorm in the ionosphere, and sometimes regarded as synonymous with "substorm onset".

Pi2 pulsations are a well-known phenomenon that is almost always observed around substorm onset as impulsive/irregular magnetic field perturbations with periods of 40–150 s. Thus, the Pi2 onset is traditionally used as a good indicator of substorm onsets. Based on numerous observational studies for about half a century [e.g., *Olson*, 1999; *Keiling and Takahashi*, 2011, and references therein], it is widely established that there is general association within a few minutes between the Pi2 onset and the auroral brightening, and Pi2 pulsations often occur on a global scale from the auroral zone to the magnetic equator across many hours of local time. However, there has still been a controversy regarding the relative timing of Pi2 to auroral brightening/expansion onset [e.g., *Kepko and McPherron*, 2001; *Liou et al.*, 2001; *Liou and Zhang*, 2009; *Murphy et al.*, 2009]. Such a controversy likely arises from differences in spatial and temporal resolution between space-based and ground-based optical instruments, or latitudinal dependence of the timings (generally, high-latitude Pi2 tends to precede low-latitude Pi2 [*Uozumi et al.*, 2000]).

A few studies have claimed that the ground Pi2 pulsations near the onset location are directly related to a quasiperiodic signature of small-scale/mesoscale preonset auroral forms observed within the field of view (FOV) of a ground-based optical camera/imager. For instance, *Solovyev et al*. [2000] and *Rae et al*. [2009] attributed the near-onset Pi2 signatures to spatial and temporal evolution of the auroral undulations of the onset arc, while *Nishimura et al*. [2012] presented that they are well correlated with quasiperiodic poleward boundary intensifications followed by equatorward propagating auroral streamer. Although some of these preonset auroral forms coexist in the vicinity of the onset site, the above observations suggested the possible linkage of the auroral-zone Pi2 magnetic signatures near the onset site to similar periodic nature of preonset aurora. However, it has not yet been established what in the preonset auroral forms causes the initial signal of the Pi2 pulsations.

Although spatial and temporal evolution of aurora is generally perceived to be similar in the Northern and Southern Hemispheres, the optical signatures often represent interhemispheric asymmetries in terms of the timing, location, and intensity. A few simultaneous optical observations of auroral substorms in both hemispheres [*Frank and Sigwarth*, 2003; *Morioka et al*., 2011], which have been very rare, indicated that the onset brightening of auroral substorm in one hemisphere precedes that in another hemisphere by ~1–2 min. Such a nonsimultaneous nature of interhemispheric auroral substorm onsets potentially suggested that the processes creating aurora operate independently in each hemisphere, presumably in/around the auroral acceleration region. However, detailed hemispheric comparison of ground Pi2 onsets near the onset region in terms of the preonset auroral evolution has not yet been done.

Recently, *Motoba et al*. [2012, hereafter "M12"] first succeeded to measure simultaneously a preonset sequence of initial brightening arc in the Northern and Southern Hemispheres, using ground-based all-sky camera (ASC) measurements at a geomagnetically conjugate pair in the auroral zone, Tjörnes (66.20°N, 342.89°E, magnetic local time (MLT) ≈ UT) in Iceland and Syowa Station (69.00°S, 39.58°E, MLT ≈ UT) in Antarctica. A detailed comparison of the interhemispheric optical images indicated that the formation and development of preonset arc were nearly identical in both hemispheres, like mirror images of each other. We note that during a few hours before this event the auroral-zone geomagnetic conditions were extremely quiet (provisional *AE* index $< 100$ nT) and consequently this auroral substorm started as an isolated activation in the ionosphere. These would be ideal conditions for determining the activation and signature of Pi wave signals around the interhemispheric onset regions. The purpose of this paper is to investigate the initiation and development of the Pi1-Pi2 band (Pi1: 1–40 s, Pi2: 40–150 s) pulsations in terms of the spatiotemporal evolution of the conjugate preonset aurora, and also their interhemispheric similarities/dissimilarities, using data from the white-light ASCs (exposure time: ~0.53 s, in this analysis the image data every 10 s were used) and magnetometers (1 s time resolution) at both stations.

## 2. Method for Identifying Pi1-Pi2 Signals

In this study, we adopt the Hilbert-Huang Transform (HHT) for decomposing the Pi1-Pi2 range signals from the ground-based magnetometer data. The HHT was originally introduced by *Huang et al*. [1998] as one of the algorithms suitable for nonlinear and nonstationary signal analysis. The application of the HHT has been widely demonstrated in the recent geophysical researches, and it has been proven to be very effective in spectrum analysis and noise filtering [cf. *Huang and Wu*, 2008]. *Kataoka et al*. [2009] recently demonstrated that the HHT method potentially allows decomposing different Pi1-Pi2 range signals from irregular geomagnetic perturbations observed at high latitudes at substorm onsets.

The HHT consists of two important parts: one is empirical mode decomposition (EMD), the other Hilbert spectral analysis. EMD is an adaptive method to identify the intrinsic oscillatory modes in terms of the characteristic time scales in the data and to decompose the data accordingly. For the HHT, the EMD is first used to decompose into a finite and small number of intrinsic mode functions (IMFs). An IMF is defined as a function satisfying the following two conditions: (1) it has the same number of zero crossings and extrema; and (2) at any point, it has symmetric envelopes defined by the local maxima and minima. Each decomposed component, the IMF, has instantaneous frequency with physical meaning. Having obtained the IMFs, the instantaneous frequency can be computed using the Hilbert spectral analysis. A more detail description of the basic method of the HHT analysis is provided by *Huang et al*. [1998].

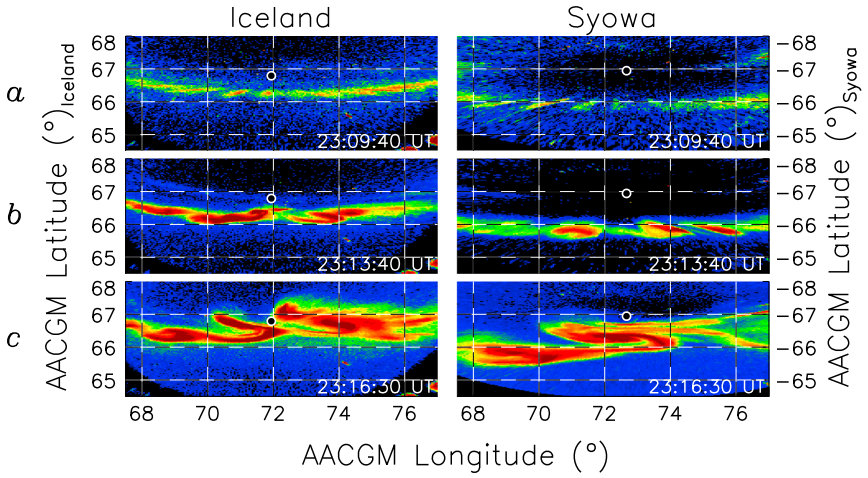


**Figure 1.** Comparison of the Iceland-Syowa auroral forms at characteristic three stages of (a) azimuthal beading, (b) spiral-like aurora, and (c) postbreakup on an arbitrary luminosity scale (Note that the color scale at the first stage (Figure 1a) is different from the other two stages (Figures 1b and 1c) to highlight a faint bead-like form). The images have been mapped in AACGM coordinates at 110 km altitude. The filled circle denotes each observatory.

## 3. Observations

### 3.1. Interhemispheric Preonset Auroral Forms

As demonstrated by M12, the conjugate preonset aurora, which occurred during an isolated substorm on 30 September 2011, underwent a two-step evolution. First, the azimuthal structuring (beading) was initiated in the preonset arc around 2308:40 UT. For about 3–4 min, the bead-like forms maintained the well-organized azimuthal structure with eastward propagation at a velocity of ~1 km $s^{-1}$. Subsequently, around 2311:30–2313:00 UT the faint, small bead-like forms with a wavelength of ~30–50 km developed into large-scale, brighter spiral-like forms. At the same time, the propagation speed became much faster (~2–6 km $s^{-1}$). After that the spiral auroral forms evolved rapidly, finally followed by auroral breakup at ~2315:30 UT. In this study, we defined as "auroral breakup" and/or "substorm onset" the time when a portion of the spiral auroral forms began to distinctly expand poleward [cf. *Mende et al*., 2009].

Figure 1 shows snapshots of the conjugate auroral images at three different stages, that is, the slowly developing stage (Figure 1a: 2309:40 UT) and active stage (Figure 1b: 2313:40 UT) of the preonset aurora, and postexpansion stage (Figure 1c: 2316:30 UT). The partial auroral images at Tjörnes in Iceland (Syowa Station), which are roughly cropped from the middle (bottom) third of the all-sky FOV, are projected in Altitude Adjusted Corrected Geomagnetic (AACGM) Coordinates [*Baker and Wing*, 1989] by assuming emissions from an altitude of 110 km. Note here that the color scale of the brightness levels is different between the first stage (Figure 1a) and the other two stages (Figures 1b and 1c), in order to highlight the faint bead-like structures at the first stage.

In Figure 1a, we can find a bead-like form characterized as the azimuthally arrayed auroral spots in the east-west auroral arc. This bead-like form was also observed with the 427.8 nm all-sky imager operated at Syowa Station (not shown here), indicating that the auroral beads were excited by the precipitation of $E >$ ~1 keV electrons. As reported by M12, the individual Iceland-Syowa beads were magnetically conjugate. The interhemispheric similarities of auroral beads suggest that the source of beads-related electrons is most likely located in the near-Earth plasma sheet. However, since each bead can be reasonably assumed to reflect the existence of localized upward field-aligned currents connecting the source region with the ionosphere, the precipitating electron energy flux sufficient to produce the fine-scale structure could be aided with an additional acceleration process in a region closer to the ionosphere. We can observe the conjugate spiral-like forms (Figure 1b), and brighter, larger-scale active aurora (Figure 1c) about 1 min after the onset. Note that the Syowa auroral forms lying far from the zenith were somewhat wider in latitude than the Iceland ones because of a geometric warping effect of the projected all-sky images. Otherwise the conjugate auroral structures at each stage were very similar.

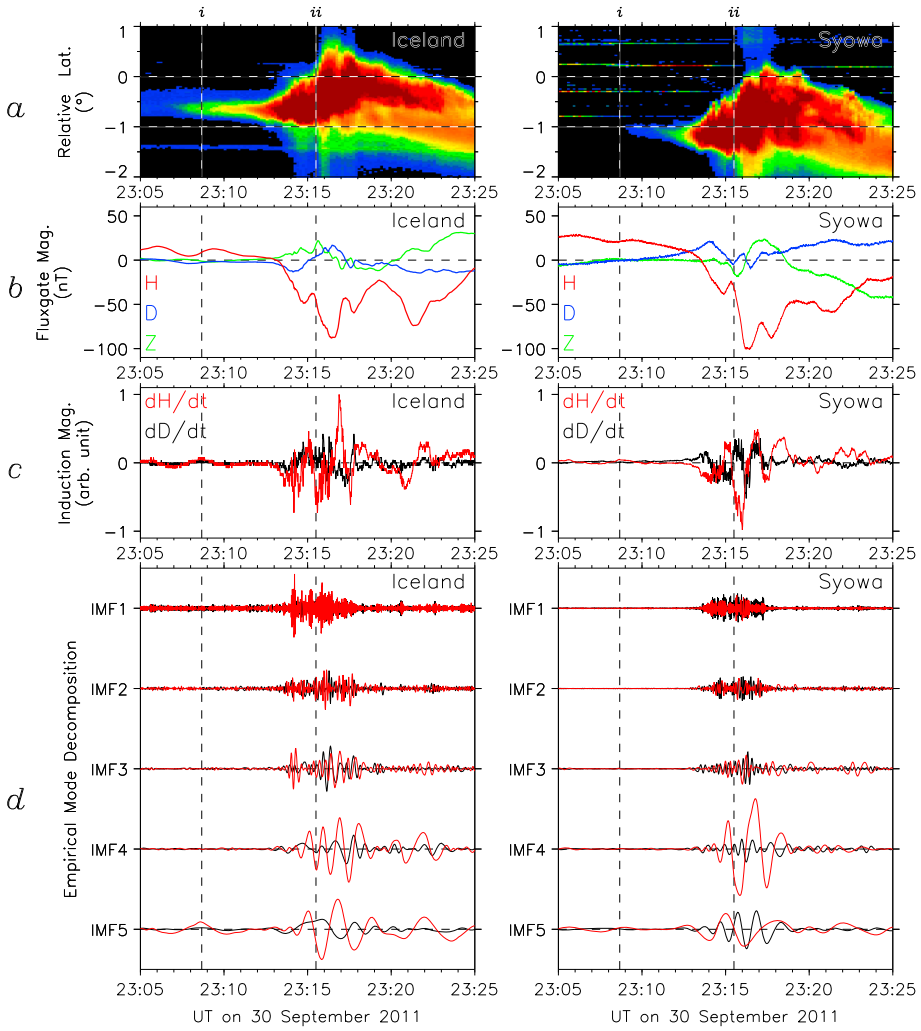


**Figure 2.** (a) Temporal variations of the Iceland (left) and Syowa (right) latitudinal profiles of auroral luminosity averaged over the longitudinal range from 69.0° to 75.0° during a 20 min interval of 2305–2325 UT. The vertical scale is labeled as relative magnetic latitude to each observatory, i.e., positive (negative) latitude means poleward (equatorward) of the observatory. (b) The *H* (red), *D* (blue), and *Z* (green) components, and (c) d*H*/d*t* (red) and d*D*/d*t* (black) components of the magnetic field. (d) First five intrinsic mode functions (IMFs) of d*H*/d*t* (red) and d*D*/d*t* (black) decomposed by empirical mode decomposition of the Hilbert spectral transform. First (i) and second (ii) vertical dashed lines denote the onsets of azimuthal beading of the preonset arc at 2308:40 UT and breakup (poleward expansion) at 2315:30 UT.

### 3.2. Relationship of Pi1-Pi2 to Preonset Arc Evolution

Figure 2 shows a detailed comparison between temporal variations of auroral keograms and magnetograms at Tjörnes in Iceland (left column) and Syowa Station (right column) for 2305–2325 UT on 30 September 2011. Two vertical dashed lines mark the onsets of (i) azimuthal structuring (beading) at 2308:40 UT and (ii) poleward expansion at 2315:30 UT. Each keogram in Figure 2a shows a latitudinal profile of the auroral luminosity averaged in the magnetic longitude range of 69°–75° and represented as a function of relative latitude to the zenith of each station (i.e., positive/negative corresponds to poleward/equatorward of observatory).
Figure 2b shows the *H* (red), *D* (blue), and *Z* (green) components of the fluxgate magnetometer data, which are in the magnetic north direction, magnetic east direction, and downward direction, respectively. Figure 2c shows the d*H*/d*t* (red) and d*D*/d*t* (black) components. Note that we used the d*H*/d*t* and d*D*/d*t* data obtained from different colocated magnetometer at each station, i.e., the induction magnetometer data at Syowa Station and the time derivative of the fluxgate magnetometer data at Tjörnes. We have compelling reasons to do so for this event: First, the induction magnetometer data were unavailable at Tjörnes; second, the time derivative of the Tjörnes fluxgate magnetometer data had relatively adequate data quality to identify minimal signals of Pi1-Pi2, allowing us to use it as an alternative for the induction magnetometer data; third,

in contrast to the Tjörnes data quality, the time derivative of the Syowa fluxgate magnetometer data suffered from a severe digital noise, probably arising from the aliasing effect in the data downsampling process. The noise prevented us from identifying the higher-frequency signals (particularly in the Pi1 range). In this study, the HHT analysis (section 2) was independently applied to the d*H*/d*t* and d*D*/d*t* components. Using the EMD, each original signal was decomposed into nine intrinsic mode functions (IMFs). The instantaneous frequencies of the first five IMFs shown in Figure 2d were within the Pi1-Pi2 range, while for the other higher modes of IMFs the frequencies were much lower than the Pi2 range. Therefore, we disregarded the higher modes of IMFs in this study.

From the auroral keograms shown in Figure 2a, it can be found that temporal behavior of the conjugate aurora was very similar at both stations through a whole interval. Note here that the conjugate auroral activity at Tjörnes in Iceland was slightly located ~0.5° poleward compared to that at Syowa Station, for which the reason will be discussed in section 4.

As mentioned above, at time (i) the first identifiable change of preonset arc began with a small-scale (~30–50 km) azimuthal beading, and then the propagating bead-like structure remained until ~2311–2312 UT. Interestingly, even as such a visible arc structuring was already in progress, no associated fluctuations can be identified in induction or fluxgate magnetometer data. Around ~2312–2313 UT, the westward auroral electrojet (i.e., negative bay in the *H* component) began to strengthen. At the same time, we can see a gradual, small increase in the *Z* component at Tjörnes in Iceland, suggesting that the westward electrojet was centered equatorward of Tjörnes. In contrast, the corresponding *Z* component change was unclear at Syowa Station. After the onset of poleward expansion (ii), the *H* component reached a minimum around 2316:30 UT, corresponding to the poleward expanding brighter aurora. Consistent with the auroral keogram, the temporal variation of the *H* component was very similar at both stations with high correlation coefficient of 0.924. For the *D* (*Z*) component, on the other hand, the Iceland-Syowa temporal variations at both stations were almost in antiphase and gave the moderate correlation coefficient of −0.793 (−0.603).

A comparison between Figures 2a and 2b shows that the latitudinal variation of aurora generally coincided with that of westward electrojet inferred from the *Z* component of the magnetic field. For instance, at the onset when the aurora activity at Tjörnes expanded poleward by crossing over the zenith, the *Z* component at Iceland decreased gradually, indicating that the overhead westward electrojet could be centered poleward of Tjörnes. Subsequently, the poleward expanded auroral activity gradually moved equatorward and after ~2320 UT the main auroral activity was located equatorward of Iceland. At the same time, the *Z* component increased again, i.e., the westward electrojet returned again to a location equatorward of Iceland. Similar tendency in the latitudinal variations of both aurora and westward electrojet was also seen at Syowa Station (the sign of *Z* component is opposite), although there was a minor difference between both stations.

With rapid evolution of preonset auroral forms around ~2312–2313 UT, magnetic field fluctuations in the Pi2 frequency started in both d*H*/d*t* and d*D*/d*t* components. About a couple of minutes later, the burst-like signals in the Pi1 frequency were superimposed. Although Pi1 is often divided into Pi1B (burst-type Pi1) and PiC (continuous-type Pi1) [*Heacock*, 1967], in this paper we refer both types as "Pi1" without any distinction. Through the whole interval, d*H*/d*t* showed a moderately correlated variation (correlation coefficient of 0.690) between the two stations, while d*D*/d*t* showed a poorly correlated variation (−0.180). The decomposed five IMFs help us to distinguish the initial Pi1-Pi2 frequency signals. The first to third components of IMFs (IMF 1, IMF 2, and IMF 3) are mainly in the Pi1 frequency range, while the forth to fifth components (IMF 4 and IMF 5) in the Pi2 frequency range. From an eye-based inspection, we found that the IMF 4 and IMF 5 signals first started at ~2312 UT and then followed by the IMF 3 signal (corresponding to long-period Pi1 $>$ 20 s). After that the IMF 1 and IMF 2 signals (corresponding to shorter-period Pi1 $<$ 20 s) were initiated. The strong Pi1-band activity remained until ~2318 UT when the breakup-related auroral luminosity decayed and the active auroral location shifted equatorward of the zenith. On the other hand, the Pi2-band activity maximized its amplitude after the onset.

Figure 3 presents time sequence of the Iceland (red) and Syowa (blue) optical intensities and their slopes, together with the Pi1-Pi2 band wave power at both stations, and the 1 min resolution *Wp* index [*Nosé et al.*, 2012] providing an indication of substorm onsets derived from middle-/low-latitude Pi2 signals using a wavelet analysis. The optical intensity at each station was averaged over the latitudinal range shown in Figure 2a.

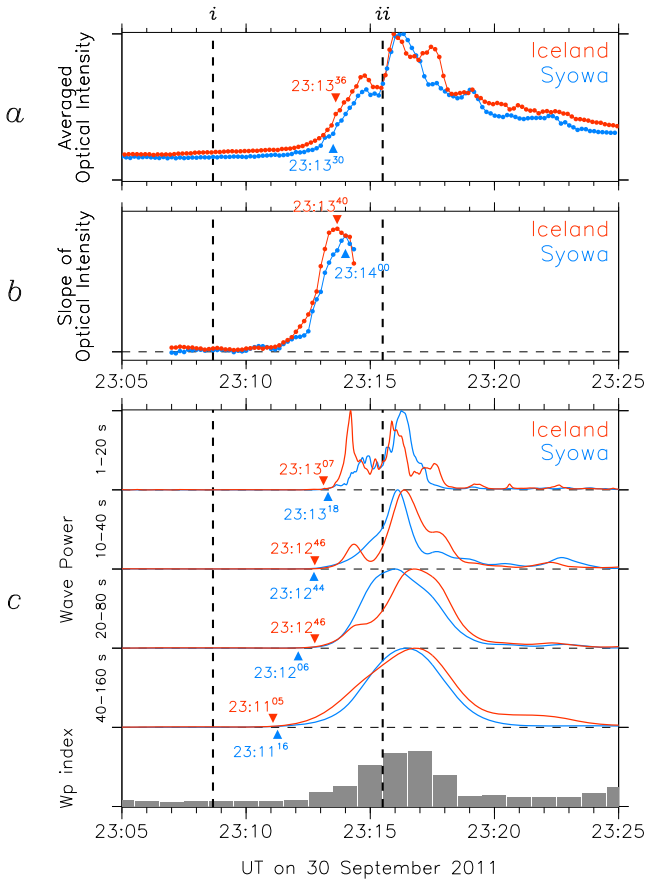


**Figure 3.** (a) Iceland (red) and Syowa (blue) auroral luminosities averaged over the latitude range shown in Figure 2a, together with the triangles marked at time when each luminosity doubles. (b) Slopes of the auroral luminosities in Figure 3a for the interval of 2307:00–2314:30 UT. Peaks of the slopes are marked by the triangles. (c) Temporal profiles of Pi1-Pi2 range wave powers and their onset times. All values are normalized by each maximum value for the time interval. Figure 3c (bottom) is *Wp* index, providing an indication of substorm onsets derived from middle-/low-latitude Pi2 signals [*Nosé et al.*, 2012]. Dashed vertical lines (i and ii) are the same as those in Figure 2.

The Pi1-Pi2 wave power was calculated by summing power in the individual period ranges of 1–20 s, 10–40 s, 20–80 s, and 40–160 s based on the IMF wave signals shown in Figure 2d. Temporal variations of the averaged auroral luminosity and Pi1-Pi2 power were normalized to each maximum value in this time interval. To help identify the preonset arc luminosity change in Figure 3a we also show the slope of optical luminosity at each time in Figure 3b, calculated from the luminosity data for ±30 s.

The color-coded solid triangles (red: Iceland, blue: Syowa) in Figure 3 represent some reference times in the auroral luminosity variation, together with the onsets of Pi1-Pi2 wave powers. The reference time in Figure 3a is set at when the arc luminosity at each station becomes twice as bright or intense as its quiet time average before 2308 UT, while in Figure 3b it is set at when the slope of the luminosity reaches a peak. In Figure 3c, the onset of each wave power determined based on an unbiased analysis method is also marked. In this method we identified the initial onset as the first enhancement of wave power values exceeding a threshold over 150 s. The threshold was defined as the mean value plus 3 standard deviations of the quiet time wave power values before 2308 UT to reduce the background noise contamination as much as possible. For this event, the threshold appears to act as a reasonable indicator of each onset because the onset apparently corresponds to the initial rise of wave powers.

As shown in Figure 3a, the Iceland-Syowa auroral luminosities underwent almost similar temporal behavior from the onset of auroral beads (i) to the onset of poleward expansion (ii), with the high correlation coefficient of 0.972. Moreover, the arc luminosity at each station varied in antiphase with the Pi2 wave cycles superimposed on the *H* component magnetic negative bay shown in Figure 2b. The correlation coefficient between the arc luminosity and magnetic *H* component variations was −0.904 at Syowa Station and −0.850 at Tjörnes in Iceland, respectively.

When taking a close look at the slope shown in Figure 3b, however, we can realize that there were some minor interhemispheric differences even in the preonset sequence. The slope change in Figure 3b would make us realize that the Iceland-Syowa auroral arc luminosity began to rise gradually around 2311 UT, although it is rather hard to identify such a small change only in Figure 3a. Consistent with such a gradual rise of arc luminosity, we could also find a structural evolution of auroral beads from a higher azimuthal wave number (*m*) of ~300–400 into a lower *m* of ~150–250 (not shown here). After that the slope of the auroral luminosity progressively steepened and then reached a peak around 2314 UT. Such a time sequence of the auroral arc luminosity variation was relatively ~20–30 s earlier at Tjörnes in Iceland than Syowa Station. Interestingly, the 40–160 s wave power (i.e., Pi2) at each station appears to take place in concert with the first noticeable slope change in the auroral luminosity, and then the wave power reached a peak around the

maximum of auroral luminosity as well as *Wp* index. The temporal variation of the 40–160 s wave power was generally identical at both stations.

On the other hand, the onset of the shorter-period waves tended to delay by ~1–2 min from the onset of the 40–160 s wave power. The onset of the rising wave power was nearly simultaneous within a time resolution of 10 s between the two stations, except for the 20–80 s wave power (time difference of ~40 s). More importantly, there existed a certain level of hemispherical differences in their subsequent temporal variations. In particular, such a hemispherical difference at the two stations was much remarkable in the shortest-period (1–20 s, i.e., Pi1) wave power even though the preonset auroral arc luminosity varied almost in a similar way: a sharp, large enhancement of 1–20 s wave power was observed at Tjörnes in Iceland, while at Syowa Station a more gradual, small enhancement was observed. In both cases, the Pi1 power enhancement appeared to be associated with a substantial enhancement in the mean arc luminosity, exceeding twice as bright as the prebeading level.

## 4. Discussion and Summary

Using the colocated optical and magnetometer observations at a geomagnetically conjugate Iceland-Syowa pair, we have presented the relationship of the initiation/development of Pi1-Pi2 pulsations near the onset location with spatiotemporal evolution of the preonset auroral arc. We found that the Iceland-Syowa optical and magnetic signatures had a certain degree of magnetic conjugacy. Of particular interest is that the first identifiable signature (i.e., precursor) in the preonset auroral arc, which began with an azimuthal bead-like formation (wavelength of ~30–50 km; wave number of ~300–400), evolved without any ground magnetic field perturbation, i.e., no Pi1-Pi2 activity. In this event, what the interhemispheric bead-like forms were very similar in terms of their formations, shapes, movements, and luminosity variations provided evidence that their source may originate in the magnetotail equatorial plane, rather than in the ionosphere. The lack of ground Pi1-Pi2 activity during the initial auroral beads may be explained in terms of the ionospheric screen effect [e.g., *Hughes and Southwood*, 1976], which prevents magnetospheric perturbations with a wavelength ~120 km from producing the magnetic signals on the ground.

Based on the observed wavelength (30–50 km) and velocity (~1 km $s^{-1}$) of the initial auroral beads, we expect the auroral beads in the ionosphere to be an oscillatory structure with a Pi1-Pi2 range periodicity of ~30–50 s if they passed overhead a fixed ionospheric point. The preonset wave activity with such a period is often observed in the near-Earth equatorial magnetotail [e.g., *Chen et al*., 2003; *Saito et al*., 2008]. The preonset low-frequency wave activity in the magnetotail is believed to result from any of potential plasma instabilities developing in a stretched near-Earth tail. Indeed, *Uritsky et al*. [2009] reported some Time History of Events and Macroscale Interactions during Substorms (THEMIS) space ground conjunction events indicating that the westward propagating preonset low-frequency wave in the near-Earth tail has common properties (e.g., scale, propagation speed, and direction) with the preonset wave-like auroral signature in the ionosphere. Their results qualitatively supported the magnetospheric drift wave modes as a possible mechanism for driving the westward propagating wave-like forms in the preonset auroral arc because the modes would propagate preferentially in the same direction as the duskward (i.e., westward) drift of higher-energy ions. It should, however, be noted again that in our event the initial bead-like forms along the arc propagated eastward at ~1 km $s^{-1}$ with maintaining the well-organized azimuthal structure. This feature completely disagrees with the above mechanism picture on the propagation direction. On the other hand, such a discrepancy raises an open question on what drives the azimuthal beading of preonset arc and what controls the propagation, which should be addressed in future preonset studies.

We have shown that the mesoscale auroral spirals were formed in concert with the Iceland-Syowa Pi2 pulsations, which is similar to examples reported by *Solovyev et al*. [2000]. However, our observations additionally indicated that the initiation of the ground Pi2 signals occurred in the transition of overhead preonset arc formation/luminosity and that the auroral arc luminosity itself oscillated coincident with the ground Pi2 wave cycles. When the Pi2 signal onset took place on the ground, the auroral beads roughly doubled in their spatial scale. These results imply that the preonset arc evolution is potentially associated with the Pi2 magnetic field signatures in the vicinity of the arc.

About 1 min after the onset of Pi2-range signals, the initial signature of Pi1-range signals was detected at the conjugate stations. As evident in Figures 2 and 3, the long-period component in the Pi1-range signals

relatively preceded the short-period one. Unlike the Pi2 activity, the Pi1 activity tends to be more spatially localized, and it may be associated with conductivity enhancements due to localized precipitation [e.g., *Grant and Burns*, 1995]. Recently, attention in the Pi1 activity has often been given to the long-period (12–48 s) signals that start relatively earlier than the other signals in the Pi1-Pi2 period range. *Milling et al*. [2008] showed that the long-period Pi1 activations are better indicator to determine the timing and location of substorm onset in the ionosphere. *Rae et al*. [2009] presented some cases that that the long-period Pi1 signals are correlated with the formation and development of small-scale auroral undulations along the substorm onset arc. Our observations have also demonstrated similar close relationship between prebreakup Pi1 activations and auroral arc undulations, except ~3–4 min interval of no ground Pi1-Pi2 activity at the early stage of auroral beading. Further analysis is required to establish the relative timing of Pi1-Pi2 activity on the ground (and in space) to the initial fine-scale structuring of preonset arc that is detectable only by high-resolution auroral imaging from the ground.

Next, we consider the interhemispheric asymmetry of the conjugate magnetic field variations at Tjörnes in Iceland and Syowa Station in Antarctica. Some minor differences can be seen in the Pi1 wave power and electrojet-related magnetic variations. In particular, from Figure 3 we found that the preonset Pi1 wave power responded differently at both stations to similar temporal variation of the conjugate auroral luminosity.

The different background properties at Tjörnes in Iceland and Syowa Station are the geomagnetic field strength and ionospheric conductance. According to the geomagnetic and ionospheric empirical models, as already mentioned by M12, the geomagnetic field strength is ~1.2 times stronger at Tjörnes than Syowa Station, while the ionospheric Pedersen conductance was ~1.5 times larger at Syowa Station than Tjörnes. The different conductance results from the difference between the geographic local times at the two stations (Syowa Station is ~4 h ahead of Tjörnes). Such interhemispheric asymmetric conditions could affect the auroral luminosity, because the resulting particle precipitation is expected to be asymmetric between both hemispheres. Unfortunately, it is not possible to make an estimate of the exact difference in the absolute auroral luminosity between both stations because of no intercharacterized optical data. It is interesting to note, however, that apparent slope changes in the relative preonset auroral luminosity at Tjörnes preceded that at Syowa Station by a few of tens seconds. A similar time difference between both stations was seen in the transition into the larger-scale spiral forms (not shown), as well as the onsets of Pi1-Pi2 power. Such a hemispheric difference might be a reflection of differences in the acceleration of precipitating auroral particles [e.g., *Morioka et al*., 2011], as well as the background conditions mentioned above, although it is inconclusive without further study.

As evident in Figures 1 and 2a, another hemispheric difference is found in the location of the conjugate aurora relative to each observatory. The auroral location at Tjörnes in Iceland was almost constantly ~0.5° poleward relative to that at Syowa Station. Such a spatial asymmetry of overhead auroral location could lead to somewhat interhemispheric difference in the local ground magnetic field perturbations at both stations because the ground magnetic field primarily arises from the integration of signals coming down from an overhead area of the ionosphere. Here we have to keep in mind that Tjörnes in Iceland and Syowa Station are not always completely the conjugate point of each other, even though there is no effect of interplanetary magnetic field on the relative displacement of both points. The latest International Geomagnetic Reference Field model predicted that the northern conjugate point of Syowa Station was located 0.47° poleward and 1.75° eastward of Tjörnes in Iceland. The predicted relative displacement in latitude reasonably agrees with the observed one. This is, of course, not an explanation but suggests that the relative latitudinal displacement of conjugate aurora to each zenith of both observatories may affect some minor hemispheric asymmetry in the Iceland-Syowa magnetic field perturbations.

In the present case study, we have investigated the interrelationship between preonset auroral and magnetic signatures during an auroral substorm observed simultaneously at a geomagnetically conjugate pair of Tjörnes in Iceland and Syowa Station in Antarctica. The major results presented here can be summarized as follows:

1. Initial formation of the preonset auroral beading for ~3–4 min evolved without any ground Pi1-Pi2 pulsations;
2. The initiation of Pi2 near the onset region appears to occur in concert with the first gradual slope change in the preonset arc luminosity just in transition from fainter auroral beads to brighter undulations, while the Pi1 onset with further enhancement in the arc luminosity being about twice as bright as the prebeading level; and

3. Pi1-Pi2 pulsations were generally similar between the conjugate stations, but there was also some dissimilarity in their temporal behaviors, which could reflect a small but noticeable interhemispheric asymmetry in the overhead conjugate preonset aurora.

Our results suggest that the initial optical signature of arc beading may potentially be a preceding indication in any preonset signatures in the onset region, like a precursor to subsequent ground Pi1-Pi2 onset and further arc brightening (namely "initial brightening"). A counterpart of the initial characteristic bead-like signature in the preonset arc, which is too small to be detected by a ground magnetometer, is presumably formed in the near-Earth tail or in the ionosphere. An interesting topic for future research is to explore what controls dynamics of the initial structuring preonset arc that leads to auroral breakup, using in situ observations in an appropriate region magnetically conjugate to the arc.

**Acknowledgments**

Work at JHU/APL was supported by the NSF grant (1104338). T.M. would like to thank T. Sakurai for helpful comments on the observed Pi1-Pi2 activity. The ground-based instrument data at Syowa Station and Iceland were provided by the National Institute of Polar Research in Japan. We acknowledge the members of the Japanese Antarctic Research Expedition supporting the continued operation of the on-site observations at Syowa Station. Icelandic ground-based observations were partially supported by a Grant-in-Aid for Scientific Research B (21403007) funded by the Ministry of education, Culture, Sports, Science and Technology of Japan. *Wp* index data were obtained from Kyoto University (http://s-cubed.info).

Robert Lysak thanks the reviewers for their assistance in evaluating this paper.

## References

Akasofu, S.-I. (1964), The development of the auroral substorm, *Planet. Space Sci.*, *12*, 273–282, doi:10.1016/0032-0633(64)90151-5.

Baker, K. B., and S. Wing (1989), A new magnetic coordinate system for conjugate studies at high latitudes, *J. Geophys. Res.*, *94*(A7), 9139–9143, doi:10.1029/JA094iA07p09139.

Chen, L.-J., A. Bhattacharjee, K. Sigsbee, G. Parks, M. Fillingim, and R. Lin (2003), Wind observations pertaining to current disruption and ballooning instability during substorms, *Geophys. Res. Lett.*, *30*(6), 1335, doi:10.1029/2002GL016317.

Frank, L. A., and J. B. Sigwarth (2003), Simultaneous images of the northern and southern auroras from the Polar spacecraft: An auroral substorm, *J. Geophys. Res.*, *108*(A4), 8015, doi:10.1029/2002JA009356.

Grant, I. F., and G. B. Burns (1995), Observations and modeling of correlated Pi B magnetic and auroral luminosity pulsations, *J. Geophys. Res.*, *100*(A10), 19,387–19,404, doi:10.1029/95JA00899.

Heacock, R. R. (1967), Two subtypes of type Pi micropulsations, *J. Geophys. Res.*, *72*(15), 3905–3917, doi:10.1029/JZ072i015p03905.

Huang, N. E., and Z. Wu (2008), A review on Hilbert-Huang transform: Method and its applications to geophysical studies, *Rev. Geophys.*, *46*, RG2006, doi:10.1029/2007RG000228.

Huang, N. E., et al. (1998), The empirical mode decomposition and the Hilbert spectrum for nonlinear and non-stationary time series analysis, *Proc. R. Soc. London*, *454*, 903–995.

Hughes, W. J., and D. J. Southwood (1976), The screening of micropulsation signals by the atmosphere and ionosphere, *J. Geophys. Res.*, *81*(19), 3234–3240, doi:10.1029/JA081i019p03234.

Kataoka, R., Y. Miyoshi, and A. Morioka (2009), Hilbert-Huang Transform of geomagnetic pulsations at auroral expansion onset, *J. Geophys. Res.*, *114*, A09202, doi:10.1029/2009JA014214.

Keiling, A., and K. Takahashi (2011), Review of Pi2 models, *Space Sci. Rev.*, *161*(1-4), 63–148.

Kepko, L., and R. L. McPherron (2001), Comment on "Evaluation of low-latitude Pi2 pulsations as indicators of substorm onset using Polar ultraviolet imagery" by K. Liou, et al, *J. Geophys. Res.*, *106*(A9), 18,919–18,922, doi:10.1029/2000JA000189.

Liou, K., and Y.-L. Zhang (2009), Comment on "Wavelet-based ULF wave diagnosis of substorm expansion phase onset" by K. Murphy et al, *J. Geophys. Res.*, *114*, A10206, doi:10.1029/2009JA014207.

Liou, K., P. T. Newell, C.-I. Meng, K. Takahashi, S.-I. Ohtani, A. T. Y. Lui, M. Brittnacher, and G. Parks (2001), Reply to comment by Kepko, L. and R. L. McPherron on "Evaluation of low-latitude Pi2 pulsations as indicators of substorm onset using Polar ultraviolet imagery", *J. Geophys. Res.*, *106*(A9), 18,923–18,926, doi:10.1029/2000JA000362.

Mende, S., V. Angelopoulos, H. U. Frey, E. Donovan, B. Jackel, K.-H. Glassmeier, J. P. McFadden, D. Larson, and C. W. Carlson (2009), Timing and location of substorm onsets from THEMIS satellite and ground based observations, *Ann. Geophys.*, *27*, 2813–2830, doi:10.5194/angeo-27-2813-2009.

Milling, D. K., I. J. Rae, I. R. Mann, K. R. Murphy, A. Kale, C. T. Russell, V. Angelopoulos, and S. Mende (2008), Ionospheric localisation and expansion of long-period Pi1 pulsations at substorm onset, *Geophys. Res. Lett.*, *35*, L17S20, doi:10.1029/2008GL033672.

Morioka, A., et al. (2011), On the simultaneity of substorm onset between two hemispheres, *J. Geophys. Res.*, *116*, A04211, doi:10.1029/2010JA016174.

Motoba, T., K. Hosokawa, A. Kadokura, and N. Sato (2012), Magnetic conjugacy of northern and southern auroral beads, *Geophys. Res. Lett.*, *39*, L08108, doi:10.1029/2012GL051599.

Murphy, K. R., I. J. Rae, I. R. Mann, A. P. Walsh, D. K. Milling, C. E. J. Watt, L. Ozeke, H. U. Frey, V. Angelopoulos, and C. T. Russell (2009), Reply to comment by K. Liou and Y.-L. Zhang on "Wavelet-based ULF wave diagnosis of substorm expansion phase onset", *J. Geophys. Res.*, *114*, A10207, doi:10.1029/2009JA014351.

Nishimura, Y., L. R. Lyons, T. Kikuchi, V. Angelopoulos, E. Donovan, S. Mende, P. J. Chi, and T. Nagatsuma (2012), Formation of substorm Pi2: A coherent response to auroral streamers and currents, *J. Geophys. Res.*, *117*, A09218, doi:10.1029/2012JA017889.

Nosé, M., et al. (2012), Wp index: A new substorm index derived from high-resolution geomagnetic field data at low latitude, *Space Weather*, *10*, S08002, doi:10.1029/2012SW000785.

Olson, J. V. (1999), Pi2 pulsations and substorm onsets: A review, *J. Geophys. Res.*, *104*(A8), 17,499–17,520, doi:10.1029/1999JA900086.

Rae, I. J., et al. (2009), Near-Earth initiation of a terrestrial substorm, *J. Geophys. Res.*, *114*, A07220, doi:10.1029/2008JA013771.

Saito, M. H., Y. Miyashita, M. Fujimoto, I. Shinohara, Y. Saito, and T. Mukai (2008), Modes and characteristics of low-frequency MHD waves in the near-Earth magnetotail prior to dipolarization: Fitting method, *J. Geophys. Res.*, *113*, A06201, doi:10.1029/2007JA012778.

Solovyev, S. I., D. G. Baishev, E. S. Barkova, N. E. Molochushkin, and K. Yumoto (2000), Pi2 magnetic pulsations as response on spatio-temporal oscillations of auroral arc current system, *Geophys. Res. Lett.*, *27*, 1839–1842, doi:10.1029/2000GL000037.

Uozumi, T., K. Yumoto, H. Kawano, A. Yoshikawa, J. V. Olson, S. I. Solovyev, and E. F. Vershinin (2000), Characteristics of energy transfer of Pi 2 magnetic pulsations: Latitudinal dependence, *Geophys. Res. Lett.*, *27*(11), 1619–1622.

Uritsky, V. M., J. Liang, E. Donovan, E. Spanswick, D. Knudsen, W. Liu, J. Bonnell, and K. H. Glassmeier (2009), Longitudinally propagating arc wave in the pre-onset optical aurora, *Geophys. Res. Lett.*, *36*, L21103, doi:10.1029/2009GL040777.